Geochemical Perspectives Letters

Bridging the depleted MORB mantle and the continental crust using titanium isotopes

Z. Deng[1]*, F. Moynier[1,2], P.A. Sossi[1], M. Chaussidon[1]

OPEN ACCESS

doi: 10.7185/geochemlet.1831

Abstract

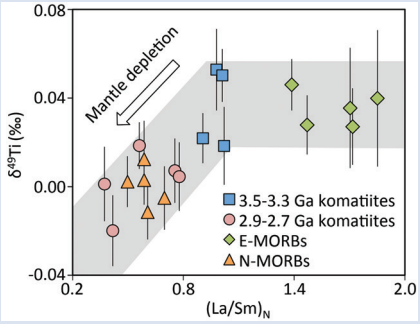

The mechanisms driving the chemical complementarity between depleted MORB mantle (DMM) and continental crust (with an average 'andesitic' composition) remain unclear. By investigating Archean komatiites, and modern enriched (E) and normal (N) MORB samples, we demonstrate that partial melting of the mantle does not fractionate Ti isotopes, whereas intracrustal differentiation causes significant Ti isotopic fractionation between melts and minerals, specifically Fe-Ti oxides. Thus, Ti isotope ratios are tracers of these two magmatic regimes. N-MORB and late Archean (2.9-2.7 Ga) komatiites are depleted in the heavier Ti isotopes compared to E-MORB and middle Archean (3.5-3.3 Ga) komatiites. We show that the depletion in the heavier Ti isotopes of the DMM is due to mantle recycling of the isotopically light residues from the generation of felsic continental crust over 3.5-2.7 Ga. This process must have reached a steady state by ≈ 2.5 Ga, based on the uniform Ti isotopic composition of contemporary N-MORBs and late Archean komatiites. This change is likely due to a decrease in the mantle potential temperature related to the emergence of plate tectonics.

Received 23 July 2018 | Accepted 27 October 2018 | Published 13 December 2018

Introduction

The Earth's mantle is chemically and isotopically heterogeneous (Allègre, 1982; Zindler and Hart, 1986). Multiple mantle end members, inferred from the radiogenic isotopic compositions (Pb-Pb, Sm-Nd and Rb-Sr) of oceanic basalts, have been defined to describe these heterogeneities (Zindler and Hart, 1986). In particular, the depleted MORB mantle (DMM), *i.e.* the inferred source of the modern normal-type mid-ocean ridge basalts (N-MORB), is characterised by a significant depletion in the incompatible trace elements (Workman and Hart, 2005), and is to a first order compositionally complementary to the continental crust (Hofmann, 1988). Thus, the DMM has been interpreted as a residual mantle that was homogenised after the extraction of a component similar to the present day continental crust (Hofmann, 1988; McCulloch and Bennett, 1994; Workman and Hart, 2005). However, since the continental crust is too silicic to have been derived from a one-step partial melting of upper mantle peridotites, the origin of its complementarity with the DMM is still unclear. Intracrustal magmatic differentiation and removal of the mafic/ultramafic complement are required to drive the bulk continental crust to andesitic compositions (Rudnick, 1995; Walter, 2003).

In order to evaluate the relationship between DMM and the continental crust, quantification of the processes causing the depletions in the incompatible trace element budget of DMM must be understood. Titanium stable isotopes are well suited to discriminate between mantle and crustal melting because they do not appear to fractionate during partial melting of the mantle, whereas they tend to become enriched in the heavier isotopes during magmatic differentiation in the crust (Millet *et al.*, 2016; Greber *et al.*, 2017a,b).

Based on the enrichments of the radiogenic Nd and Hf isotopes in N-MORB samples (Vervoort *et al.*, 1996; Vervoort and Blichert-Toft, 1999), the DMM should acquire its high Sm/Nd and Lu/Hf ratios during the late Archean. Archean komatiites are produced by high degree partial melting (25-40 %) of the mantle, and erupt at temperatures >1750 K (Arndt, 2003). These characteristics mitigate chemical and isotopic fractionations during partial melting of their sources, and therefore are sensitive records of the spatio-thermal evolution of the composition of Earth's mantle over their eruptive history (Walter, 2003; Puchtel *et al.*, 2009; Sossi *et al.*, 2016). In contrast with Archean komatiites, MORB samples are derived from lower degrees of partial melting (5-15 %) of the modern upper mantle (Asimow and Langmuir, 2003; Workman and Hart, 2005), and are subdivided based on their concentration in incompatible elements from light rare earth element depleted (N-MORB) to enriched (E-MORB) (Workman and Hart, 2005).

Here we present a high precision Ti isotopic study of Archean komatiites, and N-MORB and E-MORB. The comparison of the Ti isotopic composition of MORBs with that of Archean komatiites is used to confirm isotopic effects by partial melting of the mantle, and further trace Ti isotopic variations in the mantle since the Archean.

1. Institut de Physique du Globe de Paris, Université Paris Diderot, Université Sorbonne Paris Cité, CNRS UMR 7154, 1 rue Jussieu, 75005, Paris, France
2. Institut Universitaire de France, Paris, France
* Corresponding author (email: deng@ipgp.fr)

Results

Ti Isotopic Variations in the Archean and Modern Mantle-Derived Rocks. Individual komatiites and MORBs have δ^{49}Ti (the per mille deviation of the ^{49}Ti/^{47}Ti ratio relative to the OL-Ti standard) values between +0.053 ± 0.018 ‰ and −0.020 ± 0.016 ‰ (Tables S-1 and S-2). On average, N-MORB samples are isotopically lighter (δ^{49}Ti = +0.001 ± 0.008 ‰; 2 se, n = 5) than E-MORB samples (δ^{49}Ti = +0.035 ± 0.007 ‰; 2 se, n = 5). Similarly, among Archean komatiites, the late Archean (2.9-2.7 Ga) ones, which are depleted in incompatible trace elements, have a lower average δ^{49}Ti value (+0.003 ± 0.013 ‰, 2 se, n = 5) than the middle Archean (3.5-3.3 Ga) ones (δ^{49}Ti = +0.038 ± 0.018 ‰; 2 se, n = 4), which have primitive mantle-like trace element abundances (Fig. 1). The Ti isotopic composition of the middle Archean komatiites overlaps with the average composition of the 12 chondrite groups (δ^{49}Ti = +0.070 ± 0.054 ‰, 2 sd, n = 12; Deng *et al.*, 2018) but is lower than that of the continental crust as inferred from shale data (δ^{49}Ti = +0.181 ± 0.015 ‰, 2 se, n = 78; Greber *et al.*, 2017b) (Fig. 2). These observations imply the presence of either Ti isotopic heterogeneities in the mantle or Ti isotopic fractionations during partial melting and fractional crystallisation, or both.

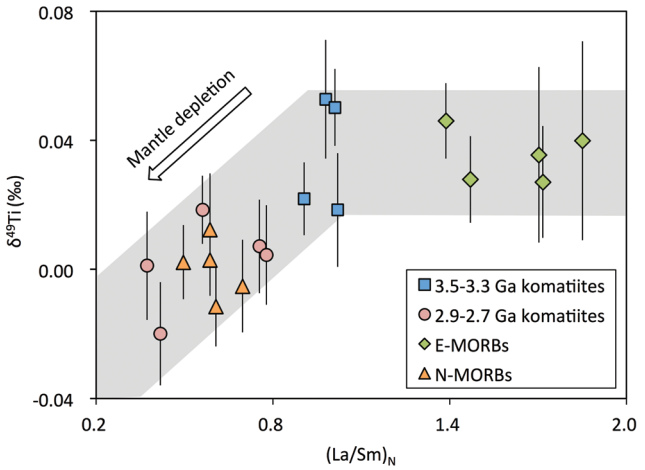

Figure 1 Positive correlation between δ^{49}Ti and $(La/Sm)_N$ values for the komatiite and MORB samples.

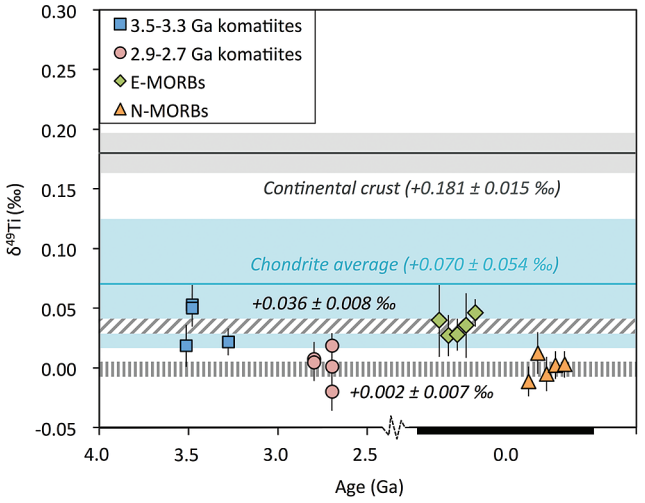

Figure 2 The change of δ^{49}Ti values with time for the komatiite and MORB samples. The average δ^{49}Ti values for the depleted and primitive groups are indicated. Also shown are the average of 12 chondrite groups with 2 sd uncertainty from Deng *et al.* (2018) and the continental crust value inferred from shale data from Greber *et al.* (2017b).

Discussion

Ti Isotopic Compositions of the Mantle Sources of Archean Komatiites. Two arguments demonstrate that Archean komatiites have inherited the Ti isotopic compositions of their mantle sources. (i) Komatiites were produced by high degree partial melting (25-40 %) at mantle potential temperature >2000 K (Arndt, 2003; Sossi *et al.*, 2016), which minimises potential Ti isotopic fractionation between komatiitic liquids and their sources. (ii) The fractional crystallisation of olivine at low pressure does not produce significant Ti isotopic fractionation in the residual melts, because Ti is incompatible in olivine (Sossi and O'Neill, 2016). Thus, the change of Ti isotopic composition of komatiites with time reflects a secular depletion in the heavier Ti isotopes of the mantle during the mid-late Archean (Fig. 2). The timing of this change in the Ti isotopic composition of the mantle matches the formation age of the DMM inferred from the Sm-Nd and Lu-Hf isotope compositions of juvenile crustal rocks of various ages (Vervoort *et al.*, 1996; Vervoort and Blichert-Toft, 1999). In addition, late Archean komatiites have a trace element inventory similar to that of the DMM (Workman and Hart, 2005; Sossi *et al.*, 2016), *e.g.*, $(La/Sm)_N$ values of 0.37-0.78 where the subscript 'N' denotes normalisation to the primitive mantle (McDonough and Sun 1995). Thus, the late Archean komatiites have likely sampled a mantle reservoir that has experienced melt extraction, potentially causing its Ti isotopic composition to trend towards that of the contemporary DMM.

Lack of Resolvable Ti Isotopic Fractionation during the Genesis of MORB Melts. Differentiated magmas tend to be enriched in the heavier Ti isotopes as a result of the preferential incorporation of the lighter Ti isotopes into the VI-fold sites of Fe-Ti oxides, relative to the lower-coordinated ones (more IV- and V-fold) of the silicate melts (Millet *et al.*, 2016). Following a similar rationale, Ti isotopes may be also fractionated during the generation of MORB melts or their subsequent differentiation. However, the magnitude of this isotopic fractionation cannot be assessed precisely from previous data or from theoretical considerations: additional experimental or theoretical work would be required to quantify these effects precisely. In the following, we estimate the magnitude of this fractionation from the present δ^{49}Ti data from the MORB and komatiite samples.

Assuming a Rayleigh distillation process for the extraction of MORB melts, which is consistent with near-fractional melting (Asimow *et al.*, 1997), the δ^{49}Ti difference of the melting residues or the partial melts relative to their sources, hereafter referred respectively as $\Delta^{49}Ti_{residue-source}$ and $\Delta^{49}Ti_{melt-source}$, should follow:

$$\Delta^{49}Ti_{residue-source} = 10^3 \times \ln\left(\alpha^{49/47}_{melt-crystal}\right) \times \ln(f) \quad \text{(Eq. 1)}$$

and

$$\Delta^{49}Ti_{melt-source} = -10^3 \times \ln\left(\alpha^{49/47}_{melt-crystal}\right) \times \ln(f) \times \frac{f}{1-f} \quad \text{(Eq. 2)},$$

where f is the remaining Ti fraction in the melting residues and $\alpha^{49/47}_{melt-crystal}$ is the melt–crystal Ti isotopic fractionation factor defined as:

$$\alpha^{49/47}_{melt-crystal} = \frac{\left(^{49}Ti/^{47}Ti\right)_{melt}}{\left(^{49}Ti/^{47}Ti\right)_{crystal}} \quad \text{(Eq. 3)}.$$

The remaining Ti fraction in the melting residues can be simply modelled by a fractional melting process:

$$f = (1-F)^{1/D_{Ti}} \quad \text{(Eq. 4)}$$

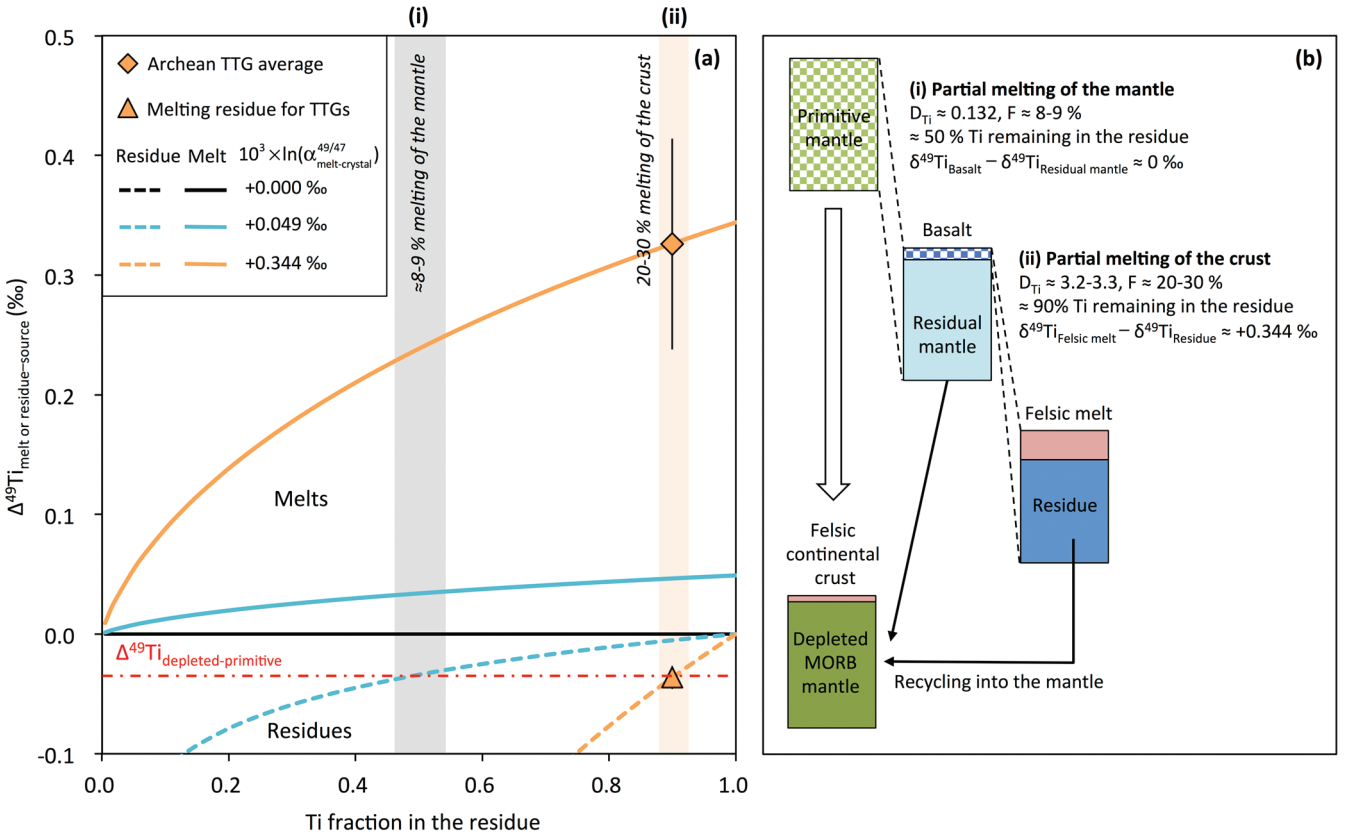

Figure 3 Modelling the Ti isotopic fractionations in the partial melts and residues from partial melting of the mantle or the crust. The grey area in **(a)** indicates the remaining Ti fraction in the residual mantle after ≈ 8-9 % partial melting (D_{Ti} ≈ 0.132; Prytulak and Elliott, 2007), *i.e.* process (i) illustrated in **(b)**. The orange field in **a** shows the Ti fraction after 20-30 % partial melting of a basaltic crust to produce the felsic melts equivalent to tonalite-trondhjemite-granodiorite (TTGs) (D_{Ti} ≈ 3.2-3.3; Martin *et al.*, 2014), *i.e.* process (ii) in **b**. The $\Delta^{49}Ti_{residue-source}$ values of TTGs and corresponding residues were calculated using the Ti isotope data of TTG samples from Greber *et al.* (2017b) and assuming E-MORBs as their sources.

where F is the melt fraction and D_{Ti} is the partition coefficient of Ti. The values of F and D_{Ti} are estimated based on experimental data. To define the value of $10^3 \times \ln(\alpha^{49/47}_{melt-crystal})$, the Ti isotopic ratios of the sources are compared to that of the partial melts or of the melting residues, *i.e.* the values of $\Delta^{49}Ti_{melt-source}$ or of $\Delta^{49}Ti_{residue-source}$ need to be determined.

During partial melting of mantle peridotites, Ti is a moderately incompatible element (D_{Ti} ≈ 0.132 for spinel peridotite; Prytulak and Elliott, 2007). The genesis of MORB melts (F = 5-15 %) should thus extract ≈ 33-71 % of the Ti from the source regions (Equation 4; Asimow and Langmuir, 2003; Workman and Hart, 2005). Using f = 0.5 (*i.e.* a mean F ≈ 8.7 %) in Equation 2, the value of $\Delta^{49}Ti_{melt-source}$ for MORBs is:

$$\Delta^{49}Ti_{melt-source} \approx 0.69 \times 10^3 \times \ln\left(\alpha^{49/47}_{melt-crystal}\right) \quad \text{(Eq. 5)}.$$

Taking the Ti isotopic compositions of the late Archean komatiites as representative of the DMM, $\Delta^{49}Ti_{melt-source}$ is equal to $\Delta^{49}Ti_{N\text{-}MORB-late\ Archean\ komatiite} = -0.002 \pm 0.015$ ‰ (2 se). This corresponds to $10^3 \times \ln(\alpha^{49/47}_{melt-crystal}) = -0.003 \pm 0.022$ ‰ (2 se) (Fig. 1).

The lack of significant Ti isotopic fractionation between crystal and melt during mantle melting raises a question about the origin of the Ti isotopic difference between the depleted and primitive mantle reservoirs ($\Delta^{49}Ti_{depleted-primitive} = -0.034 \pm 0.011$ ‰; Fig. 2). Based on its average TiO_2 content (≈ 0.119 wt. %), the DMM would be at a maximum 50 % depleted in Ti relative to the primitive mantle (≈ 0.217 wt. %) (McDonough and Sun, 1995; Workman and Hart, 2005). To produce a $\Delta^{49}Ti_{depleted-primitive} = -0.034 \pm 0.011$ ‰ would require a $10^3 \times \ln(\alpha^{49/47}_{melt-crystal})$ of +0.049 ± 0.016 ‰ using f = 0.5 in Equation 1, which is too high compared to the limited $10^3 \times \ln(\alpha^{49/47}_{melt-crystal})$ value during partial melting of the mantle peridotites (Fig. 3). Thus, another mechanism is required to explain the Ti isotopic difference between the depleted and primitive mantle reservoirs.

Recycling of Melting Residues from the Generation of the Continental Crust into the Late Archean Mantle. In contrast with the lack of melt–crystal Ti isotopic fractionation during partial melting of the peridotitic mantle, magma differentiation in the crust produces significant Ti isotopic variations (Fig. 2; Millet *et al.*, 2016; Greber *et al.*, 2017a,b). Significant volumes of felsic plutonic rocks, *i.e.* TTGs, have been generated in the late Archean (Martin, 1986). Contemporaneously, the $\delta^{49}Ti$ value of the mantle is observed to have changed, as indicated by komatiites. These TTGs likely originate from partial melting of protoliths of basaltic compositions (Martin *et al.*, 2014). Since Ti-rich minerals are stable under crustal temperatures and pressures, Ti acts as a compatible element during melt-crystal fractionation in the crust, *e.g.*, D_{Ti} ≈ 3.2-3.3 (Martin *et al.*, 2014). The generation of TTG-like melts would then extract only ≈ 10 % of Ti from the sources, using F = 0.20-0.30 and D_{Ti} = 3.2-3.3 in Equation 4. The 2.98 Ga TTGs from Kaapvaal Craton have been shown to be significantly heavier in Ti isotopes than mantle-derived rocks ($\delta^{49}Ti$ = +0.361 ± 0.088 ‰, 2 se, n = 10; Greber *et al.*, 2017b). Assuming a source with an E-MORB-like isotopic composition, these

TTGs indicate a $\Delta^{49}Ti_{melt-source} \approx +0.326 \pm 0.088$ ‰, corresponding to a $\Delta^{49}Ti_{residue-source} \approx -0.036 \pm 0.010$ ‰ and a $10^3 \times \ln(\alpha^{49/47}_{melt-crystal}) \approx +0.344 \pm 0.093$ ‰ when using $f = 0.9$ in Equations 1 and 2 (Fig. 3).

The much larger Ti isotopic fractionation produced during partial melting of crust, compared to partial melting of peridotites, likely arises from the facts that: (i) melt-crystal segregation in the crust occurs at lower temperatures (< 1273 K) than that of the normal decompression melting of the mantle (≥ 1673 K) (Martin *et al.*, 2014), and (ii) Ti is more IV- and V-fold coordinated in silicic melts than in mafic melts (Farges *et al.*, 1996). These thermal and structural differences significantly increase $10^3 \times \ln(\alpha^{49/47}_{melt-crystal})$ during the genesis of TTG-like melts. As a consequence, the residues (cumulates or restites) would be enriched in the lighter Ti isotopes with a $\Delta^{49}Ti_{residue-source} \approx -0.036 \pm 0.010$ ‰. Thus, the lighter Ti isotopic compositions of the DMM relative to the primitive mantle reservoirs could be due to mantle recycling of the residues from the generation of the late Archean felsic continental crust. To produce a $\delta^{49}Ti$ difference of 0.034 ‰ between E-MORBs and N-MORBs, an addition of ≥ 3 % shale-like sediments ($TiO_2 \approx 0.64$ wt. % and $\delta^{49}Ti \approx +0.18$ ‰; Greber *et al.*, 2017b) into the DMM ($TiO_2 \approx 0.12$ wt. % and $\delta^{49}Ti \approx +0.00$ ‰) would be needed, which is unlikely since E-MORBs have only slightly higher $^{87}Sr/^{86}Sr$ and lower $^{143}Nd/^{144}Nd$ ratios than N-MORBs (Workman and Hart, 2005). Therefore, we consider that E-MORBs are derived from a less depleted mantle reservoir that has not been subjected to crustal residue recycling rather than the one contaminated by recycled sediments.

Since the DMM ($\Delta^{49}Ti_{depleted-primitive} = -0.034 \pm 0.011$ ‰) seems to inherit the Ti isotopic composition of the residues from the formation of the late Archean TTGs ($\Delta^{49}Ti_{residue-source} \approx -0.036 \pm 0.010$ ‰; Fig. 3a), a significant proportion of Ti (94 ± 40 %) in the DMM (*i.e.* f_{Ti-DMM}) must have been processed by magma differentiation in the crust, if following the relation of $f_{Ti-DMM} = \frac{\Delta^{49}Ti_{depleted-primitive}}{\Delta^{49}Ti_{residue-source}}$. This would require that, during middle to late Archean, basaltic crust having the Ti isotopic composition of the mantle was (i) continuously extracted, and (ii) re-melted to produce a felsic continental crust, with the residues from this process being mixed into the upper mantle (Fig. 3b). The delivery of melting residues from the crust into the mantle can be achieved by either slab subduction (Martin, 1986) or lower crustal recycling (Rudnick, 1995). If the late Archean depleted mantle contained 20 % by mass of the bulk silicate Earth (BSE) (McCulloch and Bennett, 1994), the Ti isotope variations in the mantle would be produced by the extraction of a felsic continental crust constituting ≈ 0.38-0.56 % mass of the BSE during 3.5-2.7 Ga. Future Ti isotopic studies of komatiites and basalts covering the full age range of 3.5-2.7 Ga may be useful to test whether the continental extraction was continuous or abrupt. In the Archean, the hot convective mantle could homogenise the recycled melting residues into the ambient mantle. However, this mechanism should stop operating after the Archean, since the DMM was formed in the late Archean and has been stable in the upper mantle till the present day (Fig. 2). As the felsic continental crust continued to grow after the Archean (Dhuime *et al.*, 2015), additional Ti isotope heterogeneities may exist in the mantle due to the recycling of ultramafic or mafic residues from the crust, which may be later sampled by intraplate magmas. Overall, the Earth's change across the Archean-Proterozoic boundary may be due to the decrease in the thermal gradient of the mantle (Korenaga, 2013), likely signifying the prevalence of plate tectonics (Dhuime *et al.*, 2015; Tang *et al.*, 2016).

Acknowledgements

We thank John Creech for introducing IsoSpike, Manuel Moreira for providing the MORB samples, and Marc-Alban Millet for sharing OL-Ti standard. Kirsten van Zuilen is thanked for her help in the lab. FM acknowledges funding from the ERC under the H2020 framework programme/ERC grant agreement #637503 (Pristine). FM and MC thank the financial support of the UnivEarthS Labex programme at Sorbonne Paris Cité (ANR-10-LABX-0023 and ANR-11-IDEX-0005-02). Parts of this work were supported by IPGP multidisciplinary programme PARI, and by Region Île-de-France SESAME Grant no. 12015908.

Editor: Cin-Ty Lee

Additional Information

Supplementary Information accompanies this letter at http://www.geochemicalperspectivesletters.org/article1831.

Cite this letter as: Deng, Z., Moynier, F., Sossi, P.A., Chaussidon, M. (2018) Bridging the depleted MORB mantle and the continental crust using titanium isotopes. *Geochem. Persp. Let.* 9, 11–15.

References

Allègre, C.J. (1982) Chemical geodynamics. *Tectonophysics* 81, 109–132.

Arndt, N. (2003) Komatiites, kimberlites, and boninites. *Journal of Geophysical Research: Solid Earth* 108, doi: 10.1029/2002JB002157.

Asimow, P.D., Langmuir, C.H. (2003) The importance of water to oceanic mantle melting regimes. *Nature* 421, 815–820.

Asimow, P.D., Hirschmann, M.M., Stolper, E.M. (1997) An analysis of variations in isentropic melt productivity. *Philosophical Transactions of the Royal Society of London A* 355, 255–281.

Deng, Z., Moynier, F., van Zuilen, K., Sossi, P.A., Pringle, E.A., Chaussidon, M. (2018) Lack of resolvable titanium stable isotopic variations in bulk chondrites. *Geochimica et Cosmochimica Acta* 239, 409–419.

Dhuime, B., Wuestefeld, A., Hawkesworth, C.J. (2015) Emergence of modern continental crust about 3 billion years ago. *Nature Geoscience* 8, 552–555.

Farges, F., Brown Jr, G.E., Rehr, J.J. (1996) Coordination chemistry of Ti (IV) in silicate glasses and melts: I. XAFS study of titanium coordination in oxide model compounds. *Geochimica et Cosmochimica Acta* 60, 3023–3038.

Greber, N.D., Dauphas, N., Puchtel, I.S., Hofmann, B.A., Arndt, N.T. (2017a) Titanium stable isotopic variations in chondrites, achondrites and lunar rocks. *Geochimica et Cosmochimica Acta* 213, 534–552.

Greber, N.D., Dauphas, N., Bekker, A., Ptáček, M.P., Bindeman, I.N., Hofmann, A. (2017b) Titanium isotopic evidence for felsic crust and plate tectonics 3.5 billion years ago. *Science* 357, 1271–1274.

Hofmann, A.W. (1988) Chemical differentiation of the Earth: the relationship between mantle, continental crust, and oceanic crust. *Earth and Planetary Science Letters* 90, 297–314.

Korenaga, J. (2013) Initiation and evolution of plate tectonics on Earth: theories and observations. *Annual Review of Earth and Planetary Sciences* 41, 117–151.

Martin, H. (1986) Effect of steeper Archean geothermal gradient on geochemistry of subduction-zone magmas. *Geology* 14, 753–756.

Martin, H., Moyen, J.F., Guitreau, M., Blichert-Toft, J., Le Pennec, J.L. (2014) Why Archean TTG cannot be generated by MORB melting in subduction zones. *Lithos* 198, 1–13.

McCulloch, M.T., Bennett, V.C. (1994) Progressive growth of the Earth's continental crust and depleted mantle: geochemical constraints. *Geochimica et Cosmochimica Acta* 58, 4717–4738.

McDonough, W.F., Sun, S.S. (1995) The composition of the Earth. *Chemical Geology* 120, 223–253.

Millet, M.A., Dauphas, N., Greber, N.D., Burton, K.W., Dale, C.W., Debret, B., Macpherson, C.G., Nowell, G.M., Williams, H.M. (2016) Titanium stable isotope investigation of magmatic processes on the Earth and Moon. *Earth and Planetary Science Letters* 449, 197–205.

Prytulak, J., Elliott, T. (2007) TiO_2 enrichment in ocean island basalts. *Earth and Planetary Science Letters* 263, 388–403.

Puchtel, I.S., Walker, R.J., Brandon, A.D., Nisbet, E.G. (2009) Pt-Re-Os and Sm-Nd isotope and HSE and REE systematics of the 2.7 Ga Belingwe and Abitibi komatiites. *Geochimica et Cosmochimica Acta* 73, 6367–6389.

Rudnick, R.L. (1995) Making continental crust. *Nature* 378, 571–578.

Sossi, P.A., O'Neill, H.S.C. (2016) Liquidus temperatures of komatiites and the effect of cooling rate on element partitioning between olivine and komatiitic melt. *Contributions to Mineralogy and Petrology* 171, 49. doi: 10.1007/s00410-016-1260-x.

Sossi, P.A., Eggins, S.M., Nesbitt, R.W., Nebel, O., Hergt, J.M., Campbell, I.H., O'Neill, H.S.C., Van Kranendonk, M., Davies, D.R. (2016) Petrogenesis and geochemistry of Archean komatiites. *Journal of Petrology* 57, 147–184.

Tang, M., Chen K., Rudnick, R.L. (2016) Archean upper crust transition from mafic to felsic marks the onset of plate tectonics. *Science* 351, 372–375.

Vervoort, J.D., Blichert-Toft, J. (1999) Evolution of the depleted mantle: Hf isotope evidence from juvenile rocks through time. *Geochimica et Cosmochimica Acta* 63, 533–556.

Vervoort, J.D., Patchett, P.J., Gehrels, G.E., Nutman, A.P. (1996) Constraints on early Earth differentiation from hafnium and neodymium isotopes. *Nature* 379, 624–627.

Walter, M.J. (2003) Melt extraction and compositional variability in mantle lithosphere. In: Carlson, R.W. (Ed.) *Treatise on Geochemistry–The Mantle and Core*. Elsevier-Pergamon, Oxford, 363–394.

Workman, R.K., Hart, S.R. (2005) Major and trace element composition of the depleted MORB mantle (DMM). *Earth and Planetary Science Letters* 231, 53–72.

Zindler, A., Hart, S. (1986) Chemical geodynamics. *Annual Review of Earth and Planetary Sciences* 14, 493–571.

Geochemical Perspectives Letters

Bridging the depleted MORB mantle and the continental crust using titanium isotopes

Z. Deng, F. Moynier, P.A. Sossi, M. Chaussidon

Supplementary Information

The Supplementary Information includes:

- Materials
- Methods
- Supplementary Text
- Tables S-1 and S-2
- Figures S-1 and S-2
- Supplementary Information References

Materials

The Ti isotopic composition of four geological reference materials from the Geological Survey of the USA, including a Hawaiian basalt (BHVO-2), an Icelandic basalt (BIR-1), a Columbia River basalt (BCR-2) and a Guano Valley andesite (AGV-1) were analysed. Komatiites were collected from five cratons over the world (Pilbara, Kaapvaal, Zimbabwe, Yilgarn and Superior), and have eruption ages of 3.5-2.7 Ga (Table S-1). Only the freshest samples showing spinifex textures and also the chemical compositions closest to the parental magmas were chosen. Details on the samples can be found in Sossi *et al.* (2016). MORB samples from multiple mid-ocean ridges, including five N-MORB and five E-MORB, which have been studied for Cu isotopes in Savage *et al.* (2015) (Table S-1).

Methods

The powders of komatiites (≈ 100 mg) were dissolved following a Parr bomb digestion method described in Sossi *et al.* (2016). Around 11 to 48 mg rock powders of the rock standards and MORB samples were dissolved in 7 ml Savillex PFA beakers with 2 ml 26 M HF and 1 ml 16 M HNO_3 at 120 °C on a hotplate for three days. After drying down, the samples were dissolved in 3 ml 6 M HCl at 130 °C to decompose the fluorides.

The sample aliquots containing 2 to 6 µg Ti were spiked with a prepared ^{47}Ti-^{49}Ti double spike, and were then heated at 100 °C to reach sample-spike homogenisation. Afterwards, the sample solutions were dried down, and the re-dissolved sample solutions were subjected to a three-step ion-exchange chromatographic procedure, including Eichrom DGA (50-100 µm particle size) and Bio-Rad AG1-X8 (200-400 mesh) resins, to remove the matrices from Ti (Deng *et al.*, 2018). The Ti isotopic composition of the purified Ti fraction was then measured by a Thermo-Fisher Neptune multi-collector inductively-coupled-plasma mass-spectrometer (MC-ICP-MS) housed at the Institut de Physique du Globe de Paris (France). The sample solutions containing ~300 ppb of natural Ti were introduced in the MC-ICP-MS in 0.5 M HNO_3 + 0.0015 M HF *via* an APEX HF desolvating nebulizer (Elemental Scientific Inc. USA). A spiked IPGP-Ti standard was analysed in between each two analyses of unknown samples for

the secondary normalisation. The intensities of $^{44}Ca^+$, $^{46}Ti^+$, $^{47}Ti^+$, $^{48}Ti^+$ and $^{49}Ti^+$ were monitored simultaneously under a medium mass resolution (M/ΔM ≈ 5800) with a static mode. After the correction of Ca isobaric interferences, the signals of $^{46}Ti^+$, $^{47}Ti^+$, $^{48}Ti^+$ and $^{49}Ti^+$ were used for spike inversion in the IsoSpike software developed by Creech and Paul (2015). The derived data are reported with the δ-notation relative to the standards, IPGP-Ti or OL-Ti, and expressed in ‰:

$$\delta^{49}Ti_{standard} = \left[\frac{\left({}^{49}Ti / {}^{47}Ti \right)_{sample}}{\left({}^{49}Ti / {}^{47}Ti \right)_{standard}} - 1 \right] \times 1000 \qquad \text{Eq. S-1}$$

Supplementary Text

Results and inter-laboratory data comparison

Due to the presence of the small amount of isotopically fractionated Ca within the double spike, a correction of 0.022 ± 0.009 ‰ (2 se, n = 9) on the $\delta^{49}Ti_{IPGP\text{-}Ti}$ value has been conducted for all the samples. This change does not affect the isotopic difference between samples in this study. However, if aiming for high-precision inter-laboratory comparison, the analytical uncertainties of ± 0.009 ‰ from the correction of Ca effects and ± 0.011 ‰ from the calibration between IPGP-Ti and OL-Ti have to be propagated onto the corrected or re-normalised values (Deng *et al*., 2018). After all these corrections, the $\delta^{49}Ti$ values of four rock standards (BHVO-2, BIR-1, BCR-2, AGV-1), which without specification would stand for the normalization to OL-Ti standard, are consistent with the reported values in Millet *et al*. (2016) within uncertainty (Table S-1). In addition, the N-MORB samples reported here exhibit an average $\delta^{49}Ti$ value of +0.000 ± 0.008 ‰ (2 se, n = 5) or +0.000 ± 0.016 ‰ if propagating all the uncertainties above, which is in agreement with the N-MORB average value reported in Millet *et al.* (2016), *i.e*. $\delta^{49}Ti$ = +0.002 ± 0.005 ‰ (2 se, n = 7; Table S-2; Fig. S-1). These corroborate the accuracy of the method in this study.

Komatiites are characterised by a progressive depletion in both the light rare earth elements and heavy Ti isotopes with time (Figs. 1 and 2). In detail, the 3.5-3.3 Ga komatiites have $(La/Sm)_N$ values of 0.91-1.02, with subscript 'N' denoting a normalisation to the primitive mantle values from McDonough and Sun (1995), and an average $\delta^{49}Ti$ value of +0.038 ± 0.018 ‰ (2 se, n = 4). The 2.9-2.7 Ga komatiites show the lower $(La/Sm)_N$ values of 0.37-0.78 and a lower average $\delta^{49}Ti$ value of +0.003 ± 0.013 ‰ (2 se, n = 5) (Fig. 1; Table S-1). Although being reported with a larger analytical uncertainty of ± 0.035 ‰ (95 % confidence interval), similar systematics appears between the komatiite samples reported by Greber *et al*. (2017a), *i.e.* the komatiites with the primitive mantle trace element patterns tend to be isotopically heavier than depleted komatiites (Fig. S-1; Table S-2).

The average $\delta^{49}Ti$ values for chondrites in Deng *et al.* (2018) and Williams (2014) are 0.04-0.06 ‰ higher than the chondrite average in Greber *et al.* (2017a). Although the cause of the inter-laboratory discrepancy for chondrites and komatiites is not fully resolved yet (Deng *et al*., 2018), there are differences for the two analytical sessions on komatiites and chondrites in Greber *et al*. (2017a). Their first batch including most of chondrite samples has $\delta^{49}Ti$ values lower by 0.01-0.04 ‰ relative to the second batch (which includes the Allende meteorite) (Fig. S-2; Table S-2). The chondrite and komatiite data in this study, Deng *et al*. (2018) and Williams (2014) are more consistent with the results of the second batch in Greber *et al*. (2017a).

Supplementary Tables

Table S-1 Chemical and Ti isotopic compositions of komatiites and MORBs.

Sample	Location/Type/Lithology	Age (Ga)[a]	MgO (wt. %)[a]	TiO_2 (wt. %)[a]	$^{87}Sr/^{86}Sr$[b]	$(La/Sm)_N$[c]	$\delta^{49}Ti_{IPGP\text{-}Ti}$ (‰)[d]	2 s.e.[e]	2 s.e.[f]	$\delta^{49}Ti$ (‰)[g]	2 s.e.[g]	n[h]
Reference standards												
OL-Ti	Ti standard						-0.140		0.011			8
BHVO-2	basalt		9.70	0.96		1.56	-0.137	0.005	0.010	0.003	0.015	10
AGV-1	andesite		1.53	1.05		4.16	-0.049	0.012	0.015	0.090	0.019	7
BIR-1	basalt		9.70	0.96		0.37	-0.188	0.006	0.011	-0.048	0.016	26
BCR-2	basalt		3.59	2.26		2.41	-0.150	0.009	0.012	-0.011	0.017	11
Komatiites												
179/751	Pilbara Craton, Western Australia	3.515	23.54	0.42		1.02	-0.121	0.015	0.018	0.018	0.021	9
331/783	Kaapvaal Craton, South Africa	3.48	26.27	0.42		0.98	-0.087	0.016	0.018	0.053	0.022	12
331/777a	Kaapvaal Craton, South Africa	3.48	25.10	0.41		1.01	-0.089	0.008	0.012	0.050	0.016	4
176/723	Pilbara Craton, Western Australia	3.28	31.13	0.30		0.91	-0.118	0.007	0.011	0.022	0.016	3
B-R1	Zimbabwe Craton, Zimbabwe	2.8	27.72	0.29		0.75	-0.132	0.011	0.015	0.007	0.018	4
B-R2	Zimbabwe Craton, Zimbabwe	2.8	27.54	0.30		0.78	-0.135	0.013	0.015	0.005	0.019	3
SD5/354.5	Yilgarn Craton, Western Australia	2.7	25.72	0.39		0.56	-0.121	0.006	0.011	0.019	0.015	7
422/94	Superior Craton, Canada	2.7	22.41	0.45		0.42	-0.160	0.013	0.016	-0.020	0.020	6
422/95	Superior Craton, Canada	2.7	22.47	0.41		0.37	-0.138	0.014	0.017	0.001	0.020	8
Mid-ocean ridge basalts (MORBs)												
EW9309 2D-1g	Enriched-type, Mid Atlantic Ridge	≈ 0	7.60	2.04	0.704127	1.85	-0.100	0.029	0.031	0.040	0.033	6
DIVA1 15-5	Enriched-type, Mid Atlantic Ridge	≈ 0	5.93	1.16	0.703214	1.72	-0.113	0.015	0.017	0.027	0.021	7
SWIFT DR06-3-6g	Enriched-type, Southwest Indian Ridge	≈ 0	6.20	1.60	0.702900	1.47	-0.112	0.010	0.013	0.028	0.018	6
DIVA1 13-3	Enriched-type, Mid Atlantic Ridge	≈ 0	7.55	1.46	0.703000	1.70	-0.104	0.026	0.027	0.036	0.029	7
SWIFT DR04-2-3g	Enriched-type, Southwest Indian Ridge	≈ 0	6.23	1.49		1.39	-0.094	0.007	0.012	0.046	0.016	6
PAC2 DR38-1g	Normal-type, Pacific Atlantic Ridge	≈ 0	7.57	1.31	0.702465	0.61	-0.151	0.008	0.012	-0.011	0.017	6
MD57 D2-8	Normal-type, Central Indian Ridge	≈ 0	6.91	1.51		0.59	-0.127	0.015	0.017	0.012	0.021	7
SEARISE1 DR04	Normal-type, East Pacific Rise	≈ 0	5.24	1.59	0.702820	0.70	-0.145	0.011	0.014	-0.005	0.018	6
SEARISE2 DR03	Normal-type, East Pacific Rise	≈ 0	6.15	1.21		0.50	-0.137	0.007	0.011	0.002	0.016	6
RD87 DR18-102	Normal-type, Mid Atlantic Ridge	≈ 0	7.39	1.11	0.702298	0.59	-0.137	0.006	0.011	0.003	0.016	6

[a] The MgO and TiO_2 contents of the komatiites samples are from Sossi *et al*. (2016), and those of the MORB samples are from this study.

[b] The Sr isotopic ratios of the MORB samples are from the PetDB Database (http://www.earthchem.org/petdb).

[c] Subscript "N" represents the normalisation to the primitive mantle values in McDonough and Sun (1995). The $(La/Sm)_N$ values of the komatiites are from Sossi *et al*. (2016), and those of the MORBs are from this study.

[d] A correction for 0.022 ± 0.009 ‰ has been conducted for all the samples to account for the effects from the small amount of the highly isotopically fractionated Ca in the used double spike (Deng *et al*. 2018).

[e] The analytical uncertainty from the original measurement duplicates.
[f] The errors from the correction of Ca effects from double spike have been propagated.
[g] The values have been scaled onto the OL-Ti standard using the $\delta^{49}Ti_{IPGP\text{-}Ti}$ value of −0.140 ± 0.011 ‰ with error propagation.
[h] Number of measurement duplicate.

Table S-2 Literature Ti isotopic data of MORBs and mantle peridotites from Millet *et al.* (2016), komatiites (Greber *et al*., 2017a) and Archean TTGs (Greber *et al*., 2017b).

Sample	Location/Type/Lithology	Age (Ga)	MgO (wt. %)	TiO_2 (wt. %)	$(La/Sm)_N$	$\delta^{49}Ti_{IPGP\text{-}Ti}$ (‰)[d]	2 s.e.[d]	$\delta^{49}Ti$ (‰)	2 s.e.	n	Reference
Mid-ocean ridge basalts (MORBs)											
A127D8-2	Normal-type, North Atlantic	≈ 0	9.43	0.81	0.55[a]	-0.143	0.023	-0.003	0.020	1	Millet *et al.* (2016)
A127D11-1	Normal-type, North Atlantic	≈ 0	8.55	1.17	0.55[a]	-0.134	0.023	0.006	0.020	1	Millet *et al.* (2016)
R94-2	Normal-type, EPR	≈ 0	7.59	1.33	0.55[a]	-0.138	0.030	0.002	0.028	1	Millet *et al.* (2016)
R82-1	Normal-type, EPR	≈ 0	9.17	1.06	0.55[a]	-0.138	0.018	0.002	0.014	1	Millet *et al.* (2016)
Sonne12 42a	Normal-type, Pacific	≈ 0	8.23	1.50	0.55[a]	-0.135	0.024	0.005	0.021	1	Millet *et al.* (2016)
MD57 9-1	Normal-type, Indian	≈ 0	8.88	0.98	0.55[a]	-0.150	0.027	-0.010	0.025	1	Millet *et al.* (2016)
MD57 10-1	Normal-type, Indian	≈ 0	6.84	1.68	0.55[a]	-0.129	0.041	0.011	0.040	1	Millet *et al.* (2016)
Mantle peridotites											
Bch9	Alpine serpentinite	?	36.04	0.09	0.55[a]	-0.128	0.033	0.012	0.031	1	Millet *et al.* (2016)
MM15	Alpine serpentinite	?	36.34	0.06	0.55[a]	-0.143	0.030	-0.003	0.028	1	Millet *et al.* (2016)
LZ14b	Alpine serpentinite	?	38.13	0.07	0.55[a]	-0.110	0.025	0.030	0.023	1	Millet *et al.* (2016)
GP13	Beni Bousera peridotite	?	39.79	0.14	0.55[a]	-0.133	0.025	0.007	0.022	1	Millet *et al.* (2016)
Komatiites											
SCH1.1	Schapenburg	3.55	26.5	0.391	0.95	-0.135	0.032	0.005	0.030	4	Greber *et al.* (2017b)
SCH1.5	Schapenburg	3.55	25.9	0.404	0.98	-0.111	0.032	0.029	0.030	4	Greber *et al.* (2017b)
SCH1.6	Schapenburg	3.55	24.8	0.431	1.00	-0.108	0.032	0.032	0.030	4	Greber *et al.* (2017b)
SCH2.1	Schapenburg	3.55	25.2	0.428	0.94	-0.139	0.032	0.001	0.030	8	Greber *et al.* (2017b)
SCH2.2	Schapenburg	3.55	27.5	0.389	0.94	-0.104	0.032	0.036	0.030	4	Greber *et al.* (2017b)
SCH2.3	Schapenburg	3.55	27.2	0.389	0.94	-0.090	0.032	0.050	0.030	4	Greber *et al.* (2017b)
BV03	Komati	3.48	35.3	0.276	1.06	-0.131	0.032	0.009	0.030	8	Greber *et al.* (2017b)
BV04A	Komati	3.48	29.5	0.364	1.04[b]	-0.141	0.032	-0.001	0.030	4	Greber *et al.* (2017b)
BV04B	Komati	3.48	31.3	0.346	1.04[b]	-0.132	0.032	0.008	0.030	4	Greber *et al.* (2017b)
BV05	Komati	3.48	28.2	0.378	1.08	-0.118	0.032	0.022	0.030	4	Greber *et al.* (2017b)
BV06	Komati	3.48	25.3	0.434	0.99	-0.169	0.032	-0.029	0.030	4	Greber *et al.* (2017b)
564-6	Weltevreden	3.26	31.0	0.184	0.62	-0.155	0.036	-0.015	0.034	4	Greber *et al.* (2017b)
501-1b	Weltevreden	3.26	42.7	0.089	0.72	-0.136	0.035	0.004	0.033	4	Greber *et al.* (2017b)

501-2	Weltevreden	3.26	42.8	0.090	0.67	-0.162	0.032	-0.022	0.030	4	Greber *et al.* (2017b)
501-3	Weltevreden	3.26	31.0	0.177	0.67	-0.179	0.032	-0.039	0.030	4	Greber *et al.* (2017b)
501-4	Weltevreden	3.26	34.0	0.161	0.67	-0.157	0.032	-0.017	0.030	4	Greber *et al.* (2017b)
501-8b	Weltevreden	3.26	42.4	0.096	0.67	-0.141	0.035	-0.001	0.033	4	Greber *et al.* (2017b)
TN01	Belingwe	2.7	24.0	0.366	0.75[c]	-0.110	0.036	0.030	0.034	4	Greber *et al.* (2017b)
TN03	Belingwe	2.7	20.3	0.419	0.75[c]	-0.131	0.036	0.009	0.034	4	Greber *et al.* (2017b)
TN21	Belingwe	2.7	29.6	0.283	0.75[c]	-0.123	0.036	0.017	0.034	4	Greber *et al.* (2017b)
ZV10	Belingwe	2.7	27.5	0.308	0.75[c]	-0.135	0.036	0.005	0.034	4	Greber *et al.* (2017b)
ZV14	Belingwe	2.7	16.5	0.463	0.75[c]	-0.123	0.036	0.017	0.034	4	Greber *et al.* (2017b)
M657	Alexo	2.7	19.9	0.50	0.59	-0.174	0.032	-0.034	0.030	4	Greber *et al.* (2017b)
M657b	Alexo	2.7	19.9	0.50	0.59	-0.151	0.035	-0.011	0.033	4	Greber *et al.* (2017b)
M663	Alexo	2.7	28.40	0.34	0.47	-0.214	0.032	-0.074	0.030	4	Greber *et al.* (2017b)
M663b	Alexo	2.7	28.40	0.34	0.47	-0.170	0.035	-0.030	0.033	4	Greber *et al.* (2017b)
M666	Alexo	2.7	27.90	0.35	0.52	-0.200	0.032	-0.060	0.030	4	Greber *et al.* (2017b)
M666b	Alexo	2.7	27.90	0.35	0.52	-0.180	0.035	-0.040	0.033	4	Greber *et al.* (2017b)
M712	Alexo	2.7	39.60	0.21	0.60	-0.175	0.032	-0.035	0.030	4	Greber *et al.* (2017b)
M712b	Alexo	2.7	39.60	0.21	0.60	-0.140	0.035	0.000	0.033	4	Greber *et al.* (2017b)
Tonalite-trondhjemite-granodiorite (TTGs)											
96/201	Kaapvaal Craton, Murchison Belt, South Africa	2.98	0.32	0.28	6.49	0.393	0.032	0.533	0.030		Greber *et al.* (2017a)
96/202	Kaapvaal Craton, Murchison Belt, South Africa	2.98	0.40	0.21	6.06	0.430	0.032	0.570	0.030		Greber *et al.* (2017a)
96/233	Kaapvaal Craton, Murchison Belt, South Africa	2.98	0.23	0.09	7.88	0.369	0.032	0.509	0.030		Greber *et al.* (2017a)
96/246	Kaapvaal Craton, Murchison Belt, South Africa	2.98	0.70	0.31	4.94	0.204	0.032	0.344	0.030		Greber *et al.* (2017a)
96/211	Kaapvaal Craton, Rhenosterkoppies, South Africa	2.98	0.47	0.15	4.36	0.276	0.032	0.416	0.030		Greber *et al.* (2017a)
96/203	Limpopo Southern Marginal Zone, South Africa	2.98	1.64	0.29	6.32	0.126	0.032	0.266	0.030		Greber *et al.* (2017a)
96/225	Limpopo Southern Marginal Zone, South Africa	2.98	1.16	0.46	5.67	0.077	0.032	0.217	0.030		Greber *et al.* (2017a)
96/227	Limpopo Southern Marginal Zone, South Africa	2.98	1.58	0.39	3.53	0.125	0.032	0.265	0.030		Greber *et al.* (2017a)
96/217	Limpopo Southern Marginal Zone, South Africa	2.98	1.10	0.36	5.54	0.174	0.032	0.314	0.030		Greber *et al.* (2017a)
96/230	Limpopo Southern Marginal Zone, South Africa	2.98	4.69	0.60	7.25	0.033	0.032	0.173	0.030		Greber *et al.* (2017a)

[a] The MORB samples in Millet *et al.* (2016) are the normal-type, and the typical average $(La/Sm)_N$ value of 0.55 for N-MORBs is used here. The same value has been assumed for the depleted mantle peridotite samples from Millet *et al.* (2016).

[b] The average average $(La/Sm)_N$ value of the other komatiites from Komatii is shown here.

[c] The typical $(La/Sm)_N$ value of the komatiites from Belingwe in Sossi *et al.* (2016) is shown here.

[d] The values have been scaled onto the IPGP-Ti standard using the $\delta^{49}Ti_{IPGP\text{-}Ti}$ value of −0.140 ± 0.011 ‰ with error propagation.

Supplementary Figures

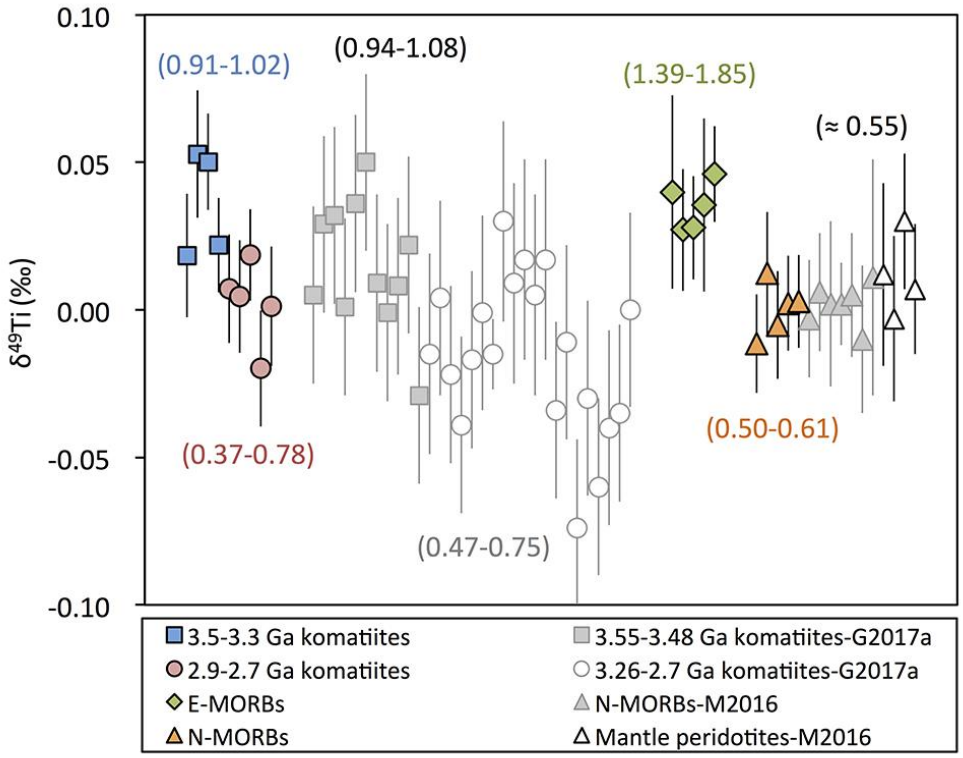

Figure S-1 Comparing the komatiite, MORB and mantle peridotite data of this study with those from Millet *et al.* (2016) and Greber *et al.* (2017a). The $(La/Sm)_N$ range of each group of samples is shown.

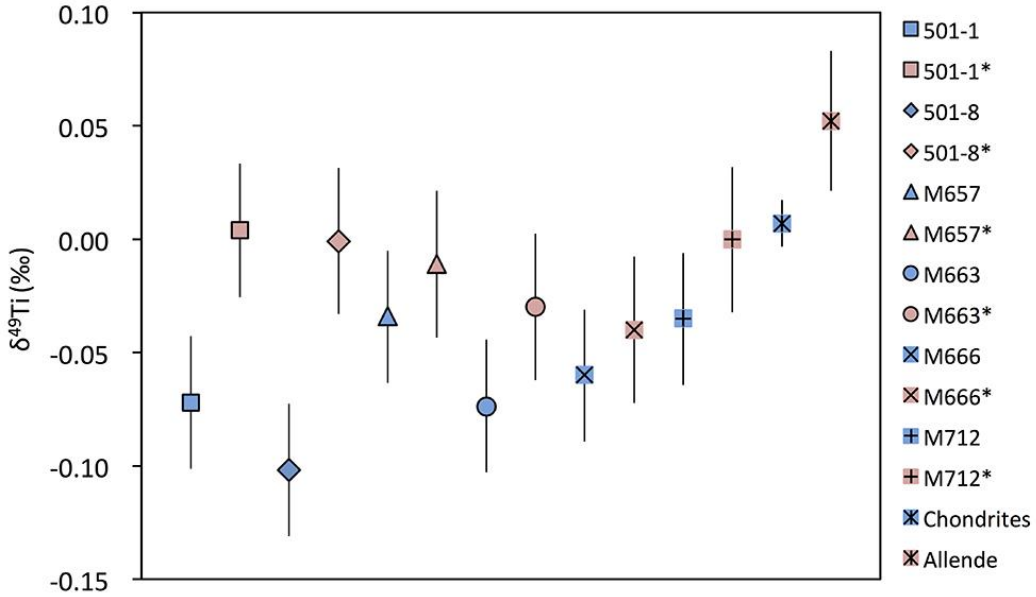

Figure S-2 Comparing the $\delta^{49}Ti$ values from two analytical sessions on chondrites and komatiites in Greber *et al.* (2017a). The first batch of dissolutions (blue labels, including most chondrites) provides the lower $\delta^{49}Ti$ values than the second batch (pink labels, including Allende meteorite).

Supplementary Information References

Creech, J.B., Paul, B. (2015) IsoSpike: Improved Double-Spike Inversion Software. *Geostandards and Geoanalytical Research* 39, 7–15.

Deng, Z., Moynier, F., van Zuilen, K., Sossi, P.A., Pringle, E.A., Chaussidon, M. (2018) Lack of resolvable titanium stable isotopic variations in bulk chondrites. *Geochimica et Cosmochimica Acta* 239, 409–419.

Greber, N.D., Dauphas, N., Puchtel, I.S., Hofmann, B.A., Arndt, N.T. (2017a) Titanium stable isotopic variations in chondrites, achondrites and lunar rocks. *Geochimica et Cosmochimica Acta* 213, 534–552.

Greber, N.D., Dauphas, N., Bekker, A., Ptáček, M.P., Bindeman, I.N., Hofmann, A. (2017b) Titanium isotopic evidence for felsic crust and plate tectonics 3.5 billion years ago. *Science* 357, 1271–1274.

McDonough, W.F., Sun, S.S. (1995) The composition of the Earth. *Chemical Geology* 120, 223–253.

Millet, M.A., Dauphas, N., Greber, N.D., Burton, K.W., Dale, C.W., Debret, B., Macpherson, C.G., Nowell, G.M., Williams, H.M. (2016) Titanium stable isotope investigation of magmatic processes on the Earth and Moon. *Earth and Planetary Science Letters* 449, 197–205.

Savage, P.S., Moynier, F., Chen, H., Shofner, G., Siebert, J., Badro, J., Puchtel, I.S. (2015) Copper isotope evidence for large-scale sulphide fractionation during Earth's differentiation. *Geochemical Perspectives Letters* 1, 53–64.

Sossi, P.A., Eggins, S.M., Nesbitt, R.W., Nebel, O., Hergt, J.M., Campbell, I.H., O'Neill, H.S.C., Van Kranendonk, M., Davies, D.R. (2016) Petrogenesis and geochemistry of Archean komatiites. *Journal of Petrology* 57, 147–184.

Williams, N.H. (2014) Titanium isotope cosmochemistry. Ph.D. thesis, Manchester University, http://www. escholar.manchester.ac.uk/uk-ac-man-scw:259269.